Effect of Surfactant on Water-Soluble Conjugated Polymer Used in Biosensor

Hameed A. Al Attar* and Andy P. Monkman

Organic Electroactive Materials Research Group, Department of Physics, University of Durham, South Road, Durham DH1 3LE, United Kingdom

Received: January 31, 2007; In Final Form: July 18, 2007

The effect of nonionic surfactants on the cationic conjugated polymer (CCP), poly{9,9-bis[6-(*N*,*N*-trimethylammonium)hexyl]fluorene-co 1,4-phenylene} iodide **1**, has been investigated. It is shown that the CCP in various solvents exists in three phases: isolated polymer chains, polymer aggregate, and variable size clusters (partially dissolved polymer). It is shown that nonionic surfactants enhance the photoluminescence (PL) quantum yield of the CCP in water by breakup of polymer aggregates, which eliminates the nonemissive interchain quenching with aggregates and increases surface-to-volume ratio of the CCP. Furthermore, the surfactants reduce quenching by incorporation of the CCP into aggregates or binary micelles. Surfactant also reduces the polar interaction strength between CCP and water and enhances CCP quenching by the counterions (iodine) by ion pairing effect. The dynamics of the interactions are complex and reveal that the surfactant induces rapid increase in the PL which imply that the main force that causes the aggregation is weak and may be due to hydrophobic interaction of the CCP in water rather than a solid, particulate-like state. Time-resolved fluorescence measurements at the exciton energy (420 nm) confirm that the CCP in water and in some organic solvents is a multiphase system in which three exponential decay terms are needed to fit the decay profile of the CCP. The change in the decay lifetime explains clearly the effect of surfactant and solvent polarity on the three CCP phases. The average lifetime of the CCP does not increase with surfactant, but the number of isolated polymer chains increases which leads to higher PL quantum yield. The association between the polymer and a quencher, single-strand deoxyribonucleic acid (ssDNA), was investigated. It indicated that CCP:ssDNA forms a weak electrostatic complex that does not alter the absorption spectra of the CCP but induces a strong CCP fluorescence quenching with association constant $K_S = 5 \times 10^7\ M^{-1}$. At low ssDNA concentrations, the surfactant reduces quenching in the complex possibly by preventing charge-transfer processes. This may be due to an increase in the distance between the CCP and ssDNA through incorporation of the CCP into aggregates (micelles). However, at high ssDNA concentration, the quenching increases sharply which may be assigned to the increase in the electrostatic force destroying the micelles' structure around the CCP, leading to contact quenching as well as DNA induced CCP aggregation, which in turn leads to CCP−CCP quenching.

Introduction

Conjugated polymers (CP) constitute a versatile class of organic materials that promise utility in a variety of applications covering electronics, optoelectronics, and electroactive devices.[1−3] The electrical, optical, and electrochemical properties of conjugated polymers can be easily modified by slightly altering their chemical structure and are strongly affected by relatively small perturbations in temperature or chemical environment. Because of this high sensitivity, conjugated polymers are promising as sensory materials.[4,5] Conjugated polymers have been used to detect chemical species (chemosensors) or biomolecules such as proteins, antibodies, and nucleotides (DNAs, RNAs, etc.), using electrical, chromic, electrochemical, and photoluminescence techniques among others. Sensing may be accomplished by transduction or amplifying physical or chemical changes into electrical, optical, or electrochemical signals. Biosensors based on conjugated polymers as sensory materials exhibit real-time response to relatively small perturbation both as fluorescent emission enhancement and as amplified fluorescence superquenching.[6] Among different chemical structures, water-soluble conjugated polymers (WSCP) is of particular interest in biosensor schemes.[7] These polymers contain charged side chain groups for solubility in aqueous media. Both cationic and anionic CPs have been synthesized and used in various biomedical applications. Recently, methods for real-time, high-sensitivity detection of polynucleotides using such WSCP were proposed.[8] Because of the conjugated hydrophobic backbones of the WSCP, the polymer has a high tendency to aggregate in an aqueous environment, which renders the material insoluble and leads to detrimental emission quenching. Several methods have been developed to increase the quantum efficiency of the WSCP by overcoming aggregation, for instance, by using site isolation utilizing branched[9] and linear[10] polymer side chains or synthesis nonionic, nonprotonic, amphiphilic polymer derivative.[11] It is known that the interaction of surfactants with WSCP leads to a dramatic increase in their fluorescent quantum yields.[12−15] The nature of the surfactant interaction with WSCP depends on the type of surfactant (cationic, anionic, or nonionic). The interaction of oppositely charged surfactants and polyelectrolytes is known to form complexes which lead to a large increase of the fluorescent quantum yields as well as to spectral change (surfactochromicity) which is used to tune the optical

* To whom correspondence should be addressed. E-mail: h.a.al-attar@durham.ac.uk.

10.1021/jp070827g CCC: $37.00
Published on Web 10/06/2007

properties of the polymers.[7,12,17−20] Surfactochromic effects and fluorescent enhancements are also observed in the interaction of nonionic surfactants with conjugated polyelectrolytes.[13,17,18] In general, the effect of the interaction of surfactant with conjugated polyelectrolytes has been explained as the following. (1) The surfactant induces breakup of polymer aggregates, eliminating interchain quenching which competes with emissive intrachain exciton relaxation that reduces the photoluminescence (PL) quantum yield.[16] (2) The surfactant induces changes to the polymer coil conformation,[12] extending the effective electron delocalization length, which leads to red spectral shifts of the absorption and emission maxima. This effect also increases the PL quantum efficiency by inhibiting the folding of the polymer chains and hence by reducing the conformational disorder and the number of kink defects, which can serve as trapping and nonradiative recombination sites. (3) Surfactants reduce fluorescence quenching by water by preventing nonradiative processes through incorporation of the polymer chains into micelles.[21,22] The interaction between the polyelectrolyte and oppositely charged surfactants is believed to be driven by a combination of electrostatic attraction and favorable entropy changes resulting from the release of interfacial water molecules.[19] Conjugated polymers and surfactants are also known to display hydrophobic interactions.[23,24] The organic core of the conjugated polymer is only partially shielded by the hydrophilic side groups; thus, hydrophobic interactions must be the dominant interaction between nonionic surfactants and cationic CP, as the electrostatic interaction does not exist. Burrows and coworkers[14,15] studied the effect of the nonionic surfactant ($C_{12}E_5$) on the properties of the anionic water-soluble poly{1,4-phenylene[9-9-bis(4-phenoxybutylsulfonate)]fluorene-2,7-diyl} copolymer (PBS−PFP) in aqueous solutions. Their results revealed that nonionic surfactants induce an increase in fluorescence quantum yields, lifetimes, and observed blue shifts of 10 nm in the absorption and emission maxima. They assign these changes to the breakup of polymer aggregates.

Dynamic and time-resolved photoluminescence (PL) could provide further insight into the interaction of the surfactant with the polyelectrolyte phases (aggregate or single-chain molecules) and on energy-transfer dynamics. However, little work has been done to study the dynamic and the time-resolved properties of the multiphase polyelectrolyte. In this work, the effect of nonionic surfactant ($C_{12}E_5$) on the percentage concentration of the cationic conjugated polymer (CCP) phases was studied. The influence of solvent polarity and hence ion pairing on the decay lifetime of CCP was also studied. Details of the steady-state photoluminescent, dynamic, and time-resolved analyses are discussed. Three exponential decay terms were found to be necessary to fit the experimental decay profile and to represent the real combination of decays that occur in the polyelectrolyte. The effect of nonionic surfactant on the CCP:ssDNA complexes was also studied, using the ssDNA oligomer as an archetypically charged quenching species.

Results and Discussion

I. Surfactant Effect on CCP Absorption and Emission Characteristics. The aqueous solution of CCP **1** (5×10^{-5} M) or 2.5×10^{-4} M per repeat unit (RU) shows broad absorption and emission bands (Figure 1) with maxima appearing at 374 and 420 nm, respectively. Upon addition of the surfactant **2** ($0-3.4 \times 10^{-4}$ M) to **1**, the absorption and fluorescent emission increases by a factor of 5 and 10 (area under the curve), respectively. The maximum surfactant concentration used exceeds by 4 times the critical micelle concentration (cmc) ($5 \pm 2 \times 10^{-5}$ M).[25,26] According to Knaapila et al.,[27] for these concentrations, our system $H_2O-CCP\ (C_{12}\ E_5)_x$ has an x value which varies from 0 to 2, that is, within the nonordered micelle regime or elongated aggregates. The measured increase in quantum yield was from $\Phi_{PL} = 0.024$ to 0.23. This increase is associated with an ~10 nm blue shift for the emission maxima, Figure 1b inset, and correspondingly little (1−2 nm) blue shift for the absorption maxima, Figure 1a inset. High concentration polymer in solution promotes chain aggregations even at high surfactant concentration and affects the blue spectral shift of both absorption and fluorescence mechanism. Furthermore, both absorption and emission exhibit spectral narrowing, and the absorption spectra show a reduction in the background absorbance (base level).

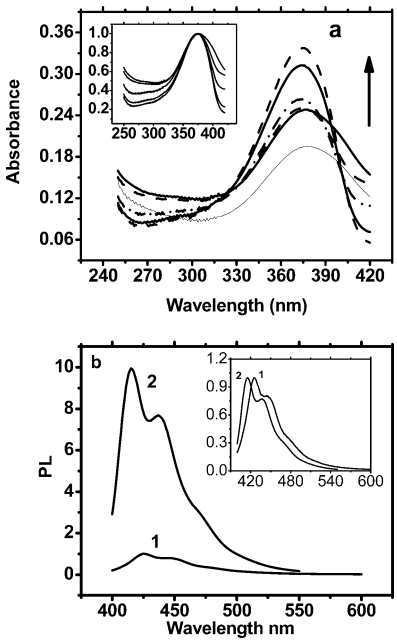

Figure 1. The effect of surfactant ($C_{12}E_5$) on the absorption (a) and emission (b) spectra of the CCP. The direction of the arrow in a indicates the change in absorbance spectra upon addition of the surfactant. Curves 1 and 2 in b are for the PL in the absence and presence of the surfactant. The normalized absorbance and emission spectral are shown in the inset. [CCP] = 1×10^{-5} M, [$C_{12}E_5$] = ($0-3.4 \times 10^{-4}$ M). $\lambda_{exc.} = 374$ nm.

These properties indicate that the surfactant induces a breakup of polymer aggregation[14] rather than being due to polymer chain conformation effects (chain extension or planarization),[12] which would be expected to induce a red shift in both the absorption and emission maxima. We would also expect this given recent elucidation of the rigid rod nature of polyfluorenes in solution.[28] The increase in absorption is due to the increase in the single-chain concentration and to a reduction in the suspended aggregated polymer particle concentration. Similar effects on the CCP were observed when we used other nonionic surfactants, Brij 35 and Triton X-100, but the PL intensity enhancement was lower and shows decay with time compared with an increase in the PL for the CCP with the $C_{12}E_5$ surfactant. This is partly due to higher molecular weight of the Brij 35 and Triton X-100 surfactants which may form heavy micelles that cause CCP/surfactant structure to precipitate. The cationic surfactants (DEAB) and (HDMAB) had almost no effect on the CCP PL emission which may ascribe to the electrostatic repulsion. The anionic surfactant (SDS) induces some emission enhancements associated with a small (4 nm) blue spectral shift, which ascribes to complexation formation.[7] Figure 2 shows the PL emission of CCP **1** and the blue shift of the emission maxima as a function

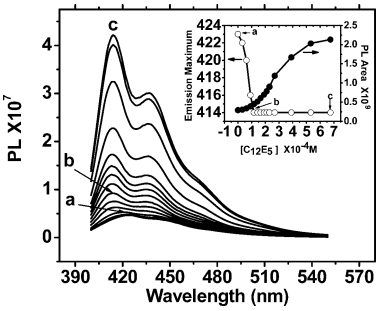

Figure 2. PL spectra of CCP (4.6×10^{-6} M) as a function of surfactant concentration ((a) 0 to (b) 1.4×10^{-4} to (c) 6.7×10^{-4} M), showing the rapid PL maximum spectral shift (a→b) and the smooth PL increase (b→c). Inset: plot of the emission maximum change and integrated PL as a function of surfactant concentration.

of the concentration of surfactant **2**. The PL emission characteristically shows a rapid blue shift (a→b) at low concentration followed by a continuous increase in PL intensity without any further spectral shift (b→c) and also shown in the inset plot. The PL intensity increases long after saturation of the blue shift and can be seen with time without addition of further surfactant. The PL characteristics of Figure 2 may vary according to the CCP molecular weight and concentration. The breakup of the polymer aggregation is assumed to induce PL enhancement by preventing interchain exciton quenching.[13] If the blue spectral shift is also related to the breakup of polymer aggregation, then the continuous increase in PL intensity with very small spectral shift should be related to another effect. An obvious effect is to incorporate the polymer into micelles (CCP/surfactant binary micelle). The cmc value for **2** in pure water is $5 \pm 2 \times 10^{-5}$ M;[25,26] however, we should assume that water containing CCP increases the cmc to some degree because of the interaction of the surfactant with CCP. Around cmc, depending on CCP concentration, we clearly see the abrupt blue shift of the emission spectrum, and the growth of intensity mainly occurs at higher surfactant concentration. In water, **2** with CCP forms elongated cylindrical micelles, which grow with concentration, temperature, or solute incorporation.[24] Knaapila et al.[27] have shown that the water/polymer (surfactant) ($D_2O-PBS-PEP$ ($C_{12}E_5$)) system realizes three phase regimes with an increasing molar ratio of surfactant over monomer unit (x). In the regime $1 \leq x \leq 2$, the solution is homogeneous and the polymer is dissolved down to the colloidal level. Small-angle neutron scattering (SANS) patterns indicate rigid elongated (polymer−surfactant) aggregates. The continuous increase in PL may be due to a collection of many effects including the further breakup of CCP, the surfactant excluding interfacial water molecules with the polymer which prevents fluorescent quenching,[29] and the surfactant changing the solvent environment. With a further increase in surfactant concentration, or over time, we envisage a growth of surfactants around the CCP spacing out the chains more and more to inhibit longer-range CCP−CCP interactions. This effect will increase the PL emission but will have no effect on the spectral shift as shown in the Figure 2 inset. To further investigate these processes, the dynamic change in PL upon addition of the surfactant was followed. The dynamics of the process was investigated by monitoring the CCP emission wavelength at 416 nm with time at excitation wavelength of 380 nm using the fluorometer operating in a fast mode. The excitation slit was set to 2 nm while the emission slit was set to 10 nm to reduce the change in the output because of the blue shift of the spectral maxima by the surfactant. The scan started with CCP in water alone and after ~20 s, 200 μL of aqueous surfactant, concentration 5×10^{-3} M, was injected into a cuvette containing 2.5 mL of aqueous CCP at a concentration of 4.6×10^{-6} M. Figure 3a shows a rapid increase in PL which is accompanied by ~8 nm blue spectral shift, stage (i) to stage (ii), followed by further increase in PL with a complete blue spectral shift to 10−12 nm in the following 5−10 s. The PL spectral Figure 3a (inset) was measured in fast mode at 10 second intervals. The final stage shows a slow increase in PL, which may relate to the slow progressive surfactant effect such as further breakup of aggregation and micelle growth as shown in Figure 3b system (iii). The rapid increase in PL from stage (i) to (ii) indicates that the main forces which cause polymer aggregation must be rather weak; we ascribe these to be weak hydrophobic interactions. The hydrophobic polymer backbones hide themselfves by forming aggregates with each other, leaving the hydrophilic soluble group in contact with the water. Upon addition of the surfactant, the hydrophobic interaction between CCP clusters and water is disrupted leading to rapid breakup of the aggregation, which was assisted by the electrostatic repulsion between the cationic groups in the CCP chains (system (ii)). This result is in the near instant increase in PL intensity via the elimination of the interchain quenching.

II. Time-Resolved Analysis. To understand in more detail the effect of the nonionic surfactant on the polyelectrolyte CCP phases, time-resolved analysis was investigated. Figure 4 shows the fluorescence decay time profile at specific surfactant concentrations. A small increase in the build in time of the PL emission is also observed in Figure 4 (inset), which may be due to geometric relaxation.[30,31] Three exponential decay functions were required to obtain a good fit to the measured data ($\chi^2 \approx 1$) in Table 1.

$$I(t) = \sum_{i=1}^{3} a_i \exp(-t/\tau_i) \tag{1}$$

where a_i represent the amplitudes of the components at $t = 0$, and τ_i is the decay time of the component i. The estimated initial (before adding surfactant) time constants obtained from the fitting of the measured decay to eq 1 were around 20, 200, and 640 ps for the CCP in water. These time constants vary upon addition of the surfactant. To characterize the three decay times, we considered two parameters. One is the fractional contribution of each component to the steady-state intensity f_i defined as[32]

$$f_i = \frac{a_i \tau_i}{\sum_j a_j \tau_j} \tag{2}$$

where the sum runs over the number of exponential terms. The terms a_i and τ_i are proportional to the area under the decay curve for each decay time. The second parameter is the fractional density of each component to the total number of fluorophores or phases α_i defined as

$$\alpha_i = \frac{a_i}{\sum_j a_j} \tag{3}$$

The two parameters were calculated for each decay component and at each surfactant concentration. The longer time constant (640 ps) is assigned to the fluorescence lifetime of the isolated polymer chains of the CCP. This decay component shows a reduction in lifetime from 640 to 570 ps upon increasing surfactant concentration; see Figure 5a and Table 1.

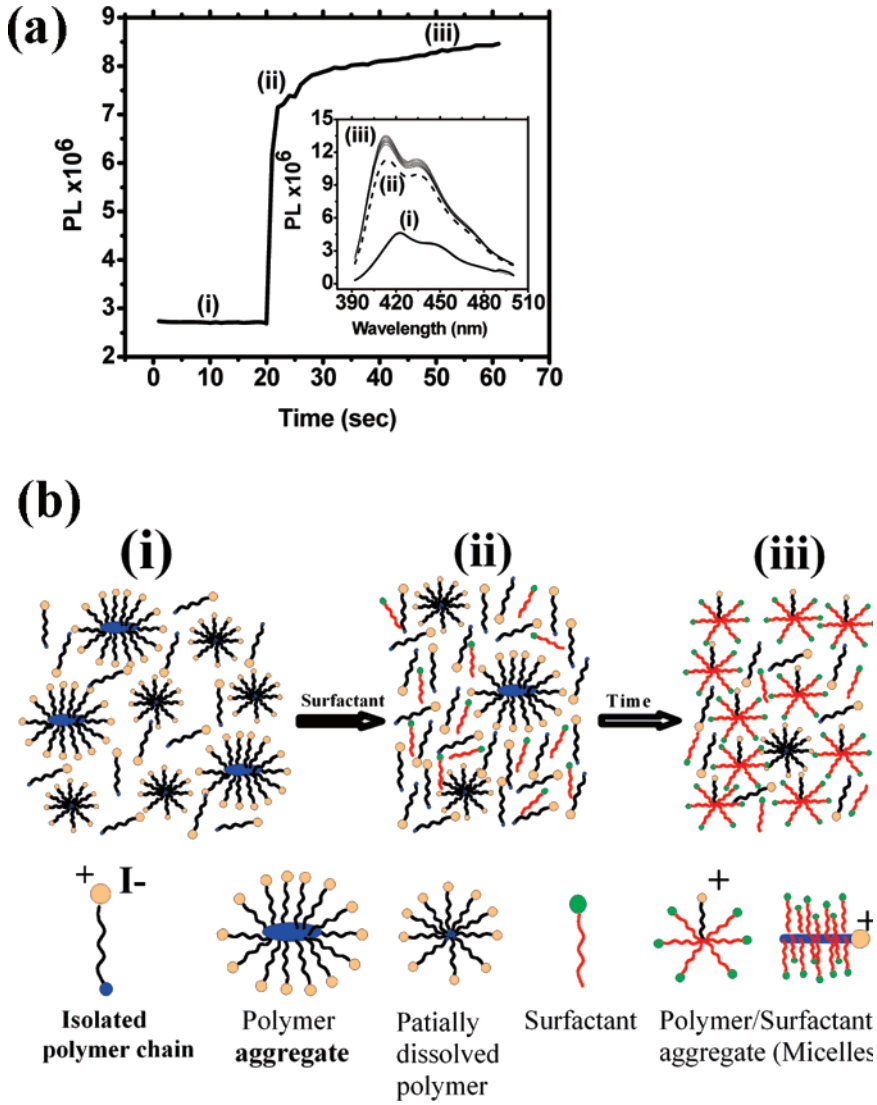

Figure 3. (a) The dynamics of PL upon addition of surfactants $C_{12}E_5$. The PL level at stage (i) is for pure CCP emission, and (ii) is the point after the addition of surfactant. (iii) is the region that slowly increases in PL with time. (b) Schematic diagram that represents the predicted system constituents in the three stages.

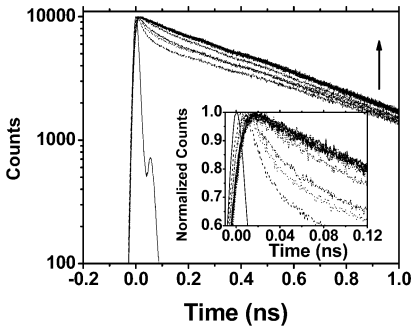

Figure 4. Selected decay time profile of the CCP 1 (5.5×10^{-5} M) in water at different surfactant concentrations (0 to 9×10^{-4} M). Inset: enlarged section showing the normal initial decay profile in normalized scale and small delay in the response. The direction of the arrow indicates the increase in surfactant concentration. $\lambda_{exc.} = 390$ nm.

This shortening of the decay time is not well understood, but it may be due to the reduction of the polarity of the water of the CCP environment by micelle formation, which screens the water−CCP interaction and reduces the relaxation time of the CCP emission.[33] The polarity reduction by the surfactant may also allow for more CCP quenching by the counterion (iodine) through an ion pairing effect.[34] Solvent polarity effects on CCP decay lifetimes for different solvents (polarity) are shown in Table 2, which confirms the reduction in the decay time of the isolated polymer chain component τ_1 with decreasing solvent polarity. Furthermore, Table 2 also shows that the contribution of this component to the steady-state PL emission, f_1, is highest, 89%, for the CCP dissolved in water, because of highest polarity, while the contribution of this component in the lowest solvent polarity (toluene) is low, 20%, and in thin film is even lower, 6.8%. This explanation may appear in contradiction with the well-known characteristics that aggregates show a red shift in the fluorescence spectra as a result of interchain interactions with long radiative lifetimes.[35] However, if the decay lifetime is measured at the blue side of the fluorescence spectra (420 nm) with the monochromator bandwidth limited to 6 nm as in our case, the decay lifetime is expected to predominantly reflect the excitons rather than interchain species (excimers, aggregates), and the influence of the interchain interactions is only to add a new branch for exciton nonradiative decay leading to "shorter" quenched exciton decay lifetime component. Therefore, the shortest decay lifetime, around 20 ps, can be assigned to the exciton decay quenched by the species in the polymer aggregate which represents lifetime

TABLE 1: The Three Time Constant Characteristics of the CCP in Water at Four Surfactant Concentrations as an Example[a]

$[C_{12}E_5]M$	a_1	τ_1	a_2	τ_2	a_3	τ_3	f_1	f_2	f_3	α_1	α_2	α_3	χ^2
0	49	644	109	17	9	203	0.89	0.054	0.05	0.29	0.65	0.05	1.1
1.92×10^{-4}	50	632	78	20	11	226	0.88	0.043	0.07	0.36	0.56	0.08	1.09
6.9×10^{-4}	54	568	33	22	15	276	0.86	0.020	0.11	0.53	0.32	0.14	1.16
0.00222	42	586	25	28	26	388	0.69	0.020	0.28	0.45	0.27	0.27	1.13

[a] a_i, τ_i, f_i, and α_i are the amplitude, time (ps), fractional contribution to the steady state, and fractional contribution to the density of phase. 1, 2, and 3 subscripts refer to the three phases (isolated polymer chain, polymer aggregate, and variable size clusters, respectively).

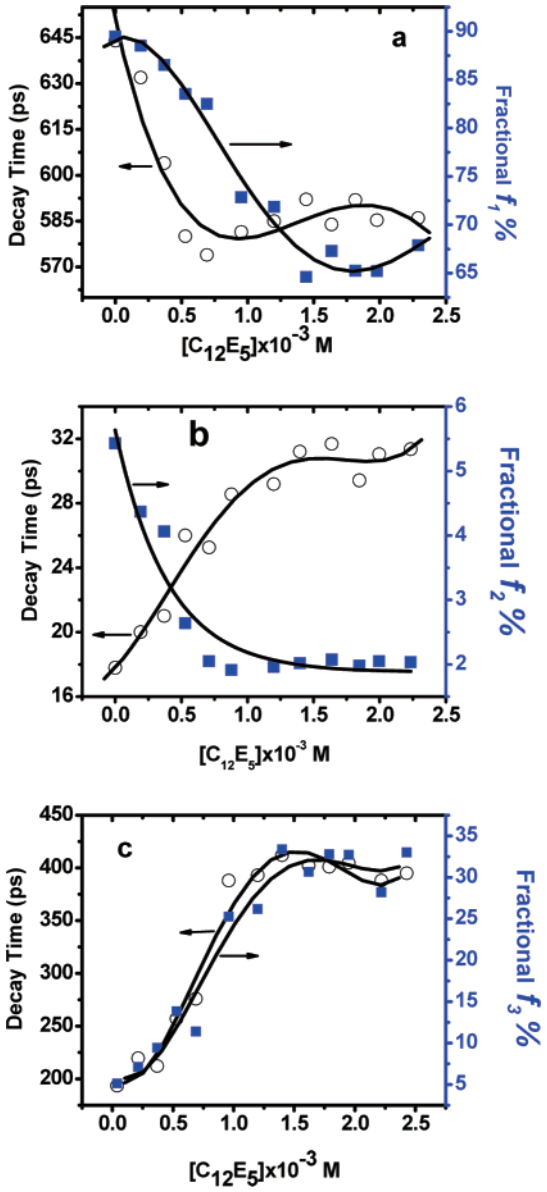

Figure 5. The variation of the three time constants and their contribution $f_i = a_i\tau_i/\Sigma\, a_i\tau_i$ to the decay profile as a function of surfactant concentration. (a) Single-chain component, (b) polymer aggregate component, and (c) cluster component. The solid lines are a guide to the eye.

quenching arising from nonradiative interchain interactions. This interchain quenching process competes with radiative intrachain exciton relaxation and reduces the overall PL intensity. The correlation between the fractional contribution of the shorter decay lifetime and the increase in PL efficiency upon addition of surfactant confirmed that this component describes the fast exciton quenching by interchain interaction in the polymer aggregate. Figure 5b shows little change in decay lifetime of this component for 18−30 ps, but most importantly the fractional contribution to the steady state, f_i, drops quickly with surfactant concentration at a rate proportional to the PL peak spectral shift. Table 2 shows that this component has very small contribution to the steady-state emission of CCP in water, 5.4%, and even lower on addition of the surfactant, 2%, see Table 1, while in thin film it is the dominant component, 70%. Table 2 also shows that higher polarity solvent dissolves more CCP than lower polarity (higher single chain phase concentration). The third intermediate decay lifetime represents variable size clusters. The larger cluster size is in the less polar solvent with shorter decay lifetime (Table 2). The smooth PL change in the CCP as the surfactant concentration increases (Figure 2, inset) appears to reflect the progressive breakup of aggregated clusters leading to an increase in the decay time from 200 to 400 ps (Figure 5c).

The increase in decay lifetime because of breakup of aggregation is higher than the reduction in decay time caused by solvatochromic and ion pairing effects because of polarity reduction leading to a resultant increase in the PL intensity with increasing surfactant concentration. This fits well with the structured data showing that the surfactant forms elongated cylindrical micelles, which grow with concentration. As the micelles thickness increases, the quenching by water and other quenchers is reduced and the PL intensity (slowly) increases. Finally, the fractional phase density of each component, α_i, as a function of concentration $[C_{12}E_5]$ is shown in Figure 6. While the density of the aggregated polymer phase is high, ~70%, this has very little impact on the steady-state intensity. As the surfactant induces breakup of the polymer aggregate, the single-chain products with longer lifetime contribute strongly to the steady-state intensity. As a_i for this component decreases, the other two components increase which confirm the transition from an aggregated polymer to clusters to isolated polymer chain. The average time that is given by

$$\langle\tau\rangle = \frac{\sum a_i\tau_i^2}{\sum a_i\tau_i}$$

remains approximately unchanged at around 450 ps.

This is because the average lifetime is dominated by the long-lived isolated polymer chain, and the aggregated polymer does not really contribute effectively to the average lifetime. The surfactant breaks up the polymer aggregation providing more isolated polymer chains, which increase the steady-state PL emission, but the average time (that is dominated by the isolated polymer chains) remains almost constant. However, a reduction in the average lifetime from 490 to 400 ps was observed as the surfactant increased, which is probably because of environmental polarity changes. The decay curves for the CCP without surfactant, Figure 4 inset, look faster for the CCP without surfactant, but that is only in the initial part of the decay, which represents the fast component. The long tail decays profile, which represents the isolated polymer chains, remains unchanged but with a higher number of counts because of a higher number of emissive isolated polymer chains. This analysis provides deeper insight into the effect of surfactant on the water-soluble conjugated polymer.

TABLE 2: The Effect of Solvent Polarity on the Decay Lifetimes and the Decay Lifetimes for Thin-Film CCP[a]

solvent	a_1	τ_1	a_2	τ_2	a_3	τ_3	f_1	f_2	f_3	α_1	α_2	α_3
water	49	644	109	18	9	203	0.89	0.054	0.051	0.29	0.65	0.053
chloroform	40	588	220	19	77	92	0.67	0.118	0.204	0.11	0.65	0.228
chlorobenzene	27	564	893	13	97	90	0.43	0.323	0.246	0.026	0.87	0.095
toluene	15	455	1204	15	146	64	0.2	0.527	0.273	0.010	0.88	0.107
thin film	6.7	352	1708	14	135	62	0.068	0.688	0.242	0.003	0.92	0.073

[a] a_i, τ_i, f_i, and α_i are the amplitude, time (ps), fractional contribution to the steady state, and fractional contribution to the density of phase. 1, 2, and 3 subscripts refer to the three phases (isolated polymer chain, polymer aggregate, and variable size clusters, respectively).

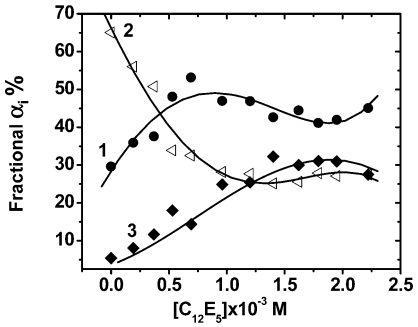

Figure 6. Fractional phase density α_i for the three components (1) isolated polymer chain, (2) polymer aggregate, and (3) clusters as a function of surfactant concentration.

III. Cationic Polyelectrolyte/Surfactant/ssDNA Complexation. One of the recent areas of interest in conjugated polyelectrolytes is their ability to be used for biosensing and drug discovery. Superquenching of fluorescence of conjugated polyelectrolytes[35,36] is one of the most promising applications. The high sensitivity of the conjugated polymers to fluorescence superquenching by small molecules suggested that superquenching might be the basis for sensitive chemical or biological application. The recent demonstration of nucleotide (DNA, RNA, etc.) sequence detection using water-soluble conjugated polymers opened a new direction for biosensor research.[30] The detection scheme depends on either Förster resonant energy transfer (FRET) from a cationic CP (CCP) as a donor to a labeled PNA or DNA as an acceptor[8] or on the conformation change of the CCP structure.[4] In both cases, the detection of specific sequence, target nucleotides depends on the hybridization condition. The hybridization condition is therefore detected by enhanced emission from the acceptor or the donor respectively. Optimization of the detection is critically important when exploring the lower concentration threshold, and selectivity is of paramount importance especially for sensing small quantities of target nucleotides or single base mismatch. In this direction, the fluorescent emission of the CCP should be maximized, while the fluorescent quenching should be minimized. In the previous section, we showed how a nonionic surfactant such as $C_{12}E_5$ improved fluorescent quantum yield. In this section, we will discuss the effect of nonionic surfactant on CCP quenching in the presence of DNA. A 12-bp ssDNA (5-ACT TGA GTT ACT-3) **3** was dissolved in water ([**3**] = 4 $\times$ 10^{-7} M). Two-and-a-half milliliters of CCP ([**1**] = 10^{-6} M) was used in a 3.5 mL cell. Similar concentrations with surfactant ([$C_{12}E_5$] = 2.3 $\times$ 10^{-4} M) were also prepared. The steady-state photoluminescence (PL) and decay profiles were measured by successive addition of ssDNA ([ssDNA] = 6.3 $\times$ 10^{-9} to 1 $\times$ 10^{-7} M). Figure 7 shows the quenching of the steady-state PL emission of the CCP without (a) and with (b) surfactant. Distinguishing characteristics in the absorption and PL emission can be seen. First, with ssDNA addition, a red shift of about 10 nm in the peak of the PL emission from 412 to 422 nm in the solution containing surfactant is observed.

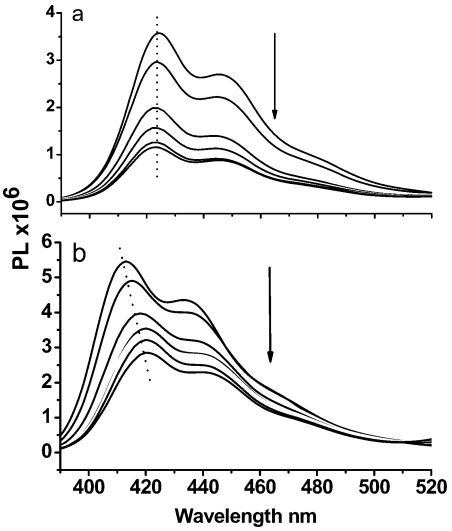

Figure 7. (a) Fluorescence spectra obtained for concentration of CCP-[1] = 10^{-6} M and DNA concentration [DNA] = 6.3 $\times$ 10^{-9} -1 $\times$ 10^{-7} M in H_2O excited at λ = 375 nm. (b) Fluorescence spectra under identical conditions but with addition of surfactant [$C_{12}E_5$] = 2.3 $\times$ 10^{-4} M. The arrow indicates the direction of increase [DNA].

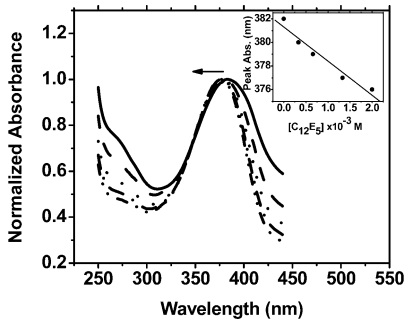

Figure 8. Surfactant-induced blue shift, spectral narrowing, and increase in molar absorption in the CCP:DNA complex. The direction of the arrow indicates the peak absorption shift by increase in surfactant concentration as shown in the inset [$C_{12}E_5$] = (3 $\times$ 10^{-4} -2 $\times$ 10^{-3} M).

This is a reverse action to the surfactant effect (induced blue shift) and indicates a contraction and aggregation of polymer chains. Second, the ssDNA induces a conformation change of the polymer in the CCP:ssDNA complex, which is confirmed by the red shift of 6$-$8 nm in the polymer absorption spectrum (374$-$382 nm). The surfactant seems to prevent this shift, to narrow the spectrum, and to increase the molar absorption by reducing the aggregation effects of the ssDNA as shown in Figure 8. However, CCP/ssDNA complexation does not show a new feature in the absorption spectra indicating that CCP:ssDNA forms a weak electrostatic complex.

Further evidence for the contribution of electrostatic complex formation is provided by the observation that increases in ionic strength significantly reduce the quenching efficiency because of ionic screening.[37] Figure 9 shows the SSC buffer concentra-

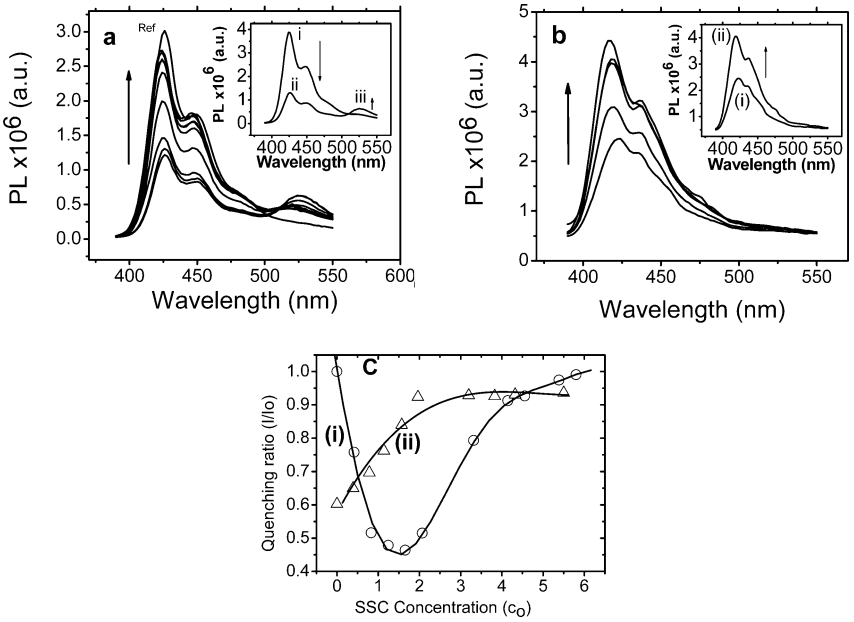

Figure 9. The photoluminescence from CCP dependence on the concentration of the SSC buffer. (a) CCP:ssDNA system, (b) CCP/surfactant:DNA system, and (c) the fluorescence quenching ratio as a function of ionic strength. The buffer concentration is in units of c_o: 1 c_o SSC buffer contains 0.15 M NaCl and 0.015 M sodium citrate, pH = 7.

tion dependence of the PL from CCP:ssDNA complex in the presence and absence of surfactant at room temperature. For CCP:ssDNA complex without surfactant, the initial addition of SSC buffer at concentrations below 1 c_o (1 c_o = 0.015 M sodium citrate and 0.15 M NaCl) causes the PL emission to be further quenched (Figure 9a inset and 9c i), and a new emission band that peaks at 525 nm appears. This may be the result of ion-induced polymer complexation/aggregation.[33] This emission band was not observed in the CCP/surfactant:DNA system (Figure 9b), and no quenching was observed (Figure 9c ii), which indicates that surfactant prevents ion-induced polymer complexation/aggregation. Further addition of SSC causes CCP emission to recover by reducing the quenching efficiencies of the CCP:ssDNA interaction through ionic screening, that is, at relatively high ionic strengths the Debye screening length is so short that polymer−DNA complex formation is inhibited.[37]

Figure 9c also indicates that surfactant reduces the binding energy of the complex as expected. Reducing the binding energy of the polymer/DNA facilitates the use of such a system in biosensing applications in which complex formation must be readily reversible at room temperature. However, the amount of surfactant is quite crucial and can be used to adjust the binding energy between the CCP and the DNA according to the biodetection methods used (superquenching or FRET).

Figure 10 shows that the quenching rate in the PL emission without surfactant is higher than that with surfactant. The quantitative description of the quenching process on addition of DNA can be represented by the Stern−Volmer equation

$$\frac{PL_0}{PL} = 1 + K_S[DNA] \qquad (4)$$

where PL_0 is the intensity of fluorescence in the absence of the quencher (ssDNA) and PL is the intensity of fluorescence in the presence of the DNA. K_S is the association constant of the static quenching through the formation of a bound complex CCP:ssDNA. As only a very weak orbital overlap between the CCP and the ssDNA exists, Dexter type charge transfer is unlikely. Two possible mechanisms may be responsible for this quenching: (1) DNA induces CCP aggregation by providing a

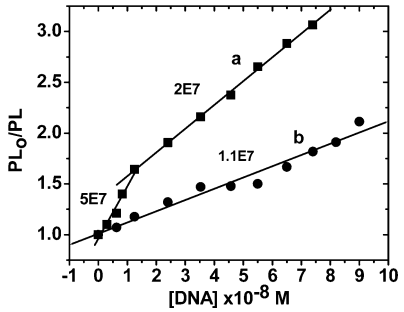

Figure 10. Stern−Volmer plot showing the quenching efficiency of the CCP/DNA complex. Fluorescence data obtained from integral spectra in Figure 7 (a) without surfactant $K_S = 5 \times 10^7$ M^{-1} and 2×10^7 M^{-1} and (b) with surfactant $K_S = 1.1 \times 10^7$ M^{-1}.

nucleation site and hence possible CCP−CCP quenching[33] and (2) CCP quenching by a charge transfer to guanine residue. The guanine with its low oxidation potential of *Eo* =1.5 V[39] may facilitate the photoinduction of charge transfer, that is, hole transfer from CCP to the DNA which resides at the guanine bases. However, the latter is not a well-understood mechanism.

Plotting PL_0/PL versus [ssDNA] and fitting the data to the Stern−Volmer equation, the association constant, K_S, calculated from the slope of the graph shown in Figure 10 is found to be dependent on the ssDNA concentration. At very low ssDNA concentrations ($<1 \times 10^{-8}$ M), the CCP is quenched very strongly by ssDNA because of complex formation with association constant $K_S = 5 \times 10^7$ M^{-1}. As ssDNA concentration increases, K_S changes to a lower value of 2×10^7 M^{-1}. These characteristics indicate that at very low ssDNA concentrations a superquenching occurs between the aggregated CCP^+ and $ssDNA^-$. As the ssDNA concentration increases, the quenching rate also decreases because of the lower availability of CCP. For the CCP/surfactant assay, the initial quenching was at a lower rate of 1.1×10^7 M^{-1}. It is suggested that the surfactant prevents CCP:ssDNA complex formation, and there may be fewer charge transfers that take place. However, in both cases, the values of K_S are extremely high and exceed that reported by Chen et al.[7] for the MPS−PPV polymer quenched by the cationic molecule methylviologen (MV^{2+}). The result shows

SCHEME 1: Chemical Structure of Water-Soluble Polyfluorene Poly{9,9-bis[*N,N*- trimethylammonium)hexyl]fluorine-co1,4-phenylene} Iodide (CCP) 1 and Its Symbolic Representative 1′ and the Nonionic Surfactant *n*-Dodecylpentaoxyethylene Glycol Ether ($C_{12}E_5$) 2 and ssDNA 3

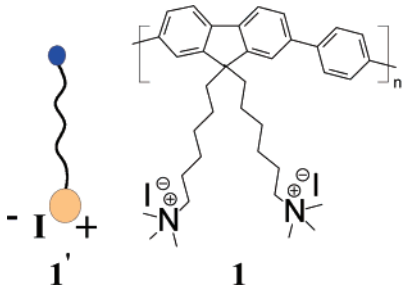

1′ 1

$H\text{-}(OCH_2CH_2)_5OCH_2(CH_2)_{10}CH_3$
$(C_{12}E_5)$
2

ssDNA : 5′-ACT TGA GTT ACT-3′
3

that the fluorescence of the CCP is quenched by the presence of very small amounts of ssDNA and upon incorporation of surfactant; this quenching is reduced by a factor of 5. This is most probably because of increasing the distance between the CCP and the ssDNA via micelle formation, which reduces possible charge-transfer mechanisms. However, the strong quenching observed in the presence of the surfactant (Figure 10b) indicates that CCP−CCP aggregation by nucleation on the ssDNA has an extremely high impact on the overall quenching mechanism.

Charge transfer is a short-range process, which is estimated to be effective for a mean distance of less than 10 Å for the MPS−PPV quenched by the cationic molecule methylviologen (MV^{2+}).[37] This short range can be screened completely by micelle formation. On the other hand, the long-range electrostatic interaction between CCP and DNA is still effective leading to CCP aggregation and therefore to possible CCP−CCP quenching. We believe that the high quenching of the CCP fluorescence in the presence of ssDNA is due to both charge transfer[7] and CCP−CCP quenching.[33] However, at relatively high ssDNA concentration [ssDNA] $> 1 \times 10^7$ M, a strong increase in the CCP quenching was observed (not shown in Figure 9), and this is probably because of the increase in the electrostatic force between CCP and ssDNA leading to collapse in the micelle structure around the CCP.

Conclusion

Nonionic surfactant enhances the photoluminescence of the water-soluble conjugated polymers by breaking up polymer aggregates and by incorporating the polymer chain into micelles. The force that holds the cationic CP in an aggregate in solution is not well understood, but the dynamic fluorescent results indicate that the main force is weak, and we believe it to be due to a hydrophobic interaction. Surfactant weakens the hydrophobic force causing a rapid breakup of polymer aggregation and instant increase in CCP fluorescence quantum yield. Time-resolved measurements are able to describe the interchain species effect on the exciton lifetime and hence on the overall quantum yield efficiency that changes dramatically by solvent polarity and nonionic surfactant.

The fluorescence of the CCP can be quenched by very small amounts of ssDNA molecules. These "superquenching" properties can be used in detecting minor alterations in the ssDNA properties. The quenching is found to arise from more than one mechanism, that is, aggregation and complexation. Surfactant reduces the aggregation or the complex binding energy and hence reduces the short-range charge-transfer contribution while sustaining the long-range electrostatic interaction. This effect enhances DNA sequence detection when a relatively long-range FRET process is sustained while the quenching of CCP by short-range charge transfer in nonselective DNA is minimized. The sensitivity and selectivity of specific DNA sequence detection in polymer/surfactant system is to be published elsewhere.

Experimental Methods

The cationic water-soluble conjugated polymer (CCP) poly-{9,9-bis[6-(*N,N*-trimethylammonium)hexyl]fluorine-co 1,4-phenylene} iodide **1** (Scheme 1), molecular weight ca. 3000 g/mol, was synthesized at the University of Wuppertal.[39] The nonionic *n*-dodecylpentaoxyethylene glycol ether ($C_{12}E_5$) **2** was purchased from Aldrich and was diluted to the required concentration using distilled and deionized water (Millipore filtration system 18 MΩ/□), and for solvent polarity effect, some organic solvents such as chlorobenzene (CB), chloroform (CF), and toluene (T) were used.

Other nonionic surfactants such as Brij 35 ($C_{12}E_{23}$) and Triton X-100 and anionic surfactants like sodium dodecyl sulfate (SDS) and cationic surfactants like dodecylethyldimethyl-ammonium bromide (DEAB) and hexadecyl-trimethylammonium bromide (HDMAB) were also studied for comparison. The interaction between the CCP and DNA in the presence of the surfactant was achieved using a 12 bp single-strand DNA (ssDNA) (5-ACT TGA GTT ACT-3) **3** purchased from MWG Biotech dissolved in 10 mM phosphate buffer ([**3**] $= 4 \times 10^{-7}$ M).

The absorption and the PL emission spectra of the conjugated polyelectrolyte CCP and of the mixtures of CCP/surfactant or CCP/surfactant/DNA were measured using a Perkin-Elmer Lambda 19 spectrophotometer and a Jobin Yvom Fluorolog spectrofluorometer, respectively. The method used to determine the photoluminescence quantum yield (PLQY) is a comparative method. The luminescence standard used as a reference was 9,10-diphenyl anthracene (DPA), and in ethanol its PLQY is 0.95.[40] Because of the suspension properties of the CCP in water, the measurement of the optical density cannot determined accurately because of multiple scattering. To overcome this problem, the absorbance in a 1 cm cuvette (i.e., optical density (OD)) for a set of concentrations 0.01−0.1 M were measured in the wavelength range 300−450 nm. The scattering background was eliminated by subtraction of the OD values at 450 or 300 nm (where the absorbance reaches steady value) from the whole absorbance spectra (there is negligible wavelength dependence at the two ends of the spectra). The corrected OD values were plotted, and the linear region at low concentration was extrapolated to determine the concentration at OD = 0.005. The PL intensity at this concentration was measured, and the PLQY relative to DPA was calculated. As we added the surfactant, the scattering value decreased and the absorbance increased and more accurate measurement could be achieved. Time-resolved fluorescence decays were collected using the picosecond time-correlated single-photon-counting (TCSPC)

technique (IRF = 12 ps). The excitation source is a picosecond Ti:Sapphire laser from (MIRA) Coherent Inc. (vertical polarization, wavelength range: 720−1000 nm, 76 MHZ repetition rate) coupled to a second-harmonic generator (360−500 nm). Emission collected at the magic-angle polarization is detected through a double subtractive monochromator by a microchannel plate (MCPT) Hamamatsu model R3809U-50. Signal acquisition was performed using a TCSPC module (Becker & Hickl Model SPC-630). Deconvolution of the fluorescence decays was performed using Globals WE software package.[41] To analyze the influence of surfactant on the decay lifetime of the CCP, we used the single-photon-counting system in high-resolution mode (0.8 ps/channel), and the collected peak counts were greater than 12 000 counts.

Acknowledgment. The authors thank Professor Ulli Scherf for the kind gift of the cationic conjugated polymer CENAMPS for funding via the Durham University Photonic Materials Institute.

References and Notes

(1) Skotheim, T. A.; Reynolds, J.; Elsenbaumer, R. *Handbook of Conducting Polymers;* Dekker: New York, 1998.

(2) Friend, R. H.; Gymer, R. W.; Holmes, A. B.; Burroughes, J. H.; Marks, R. N.; Taliani, C. D.; Bradley, D. C.; Dos Santos, D. A.; Bredas, J. L.; Longdlund, M.; Salaneck, W. R. *Nature (London)* **1999**, *397*, 121.

(3) McGehee, M. D.; Miller, E. K.; Moses, D.; Heeger, A. J. In *Twenty Years of Conducting Polymers: From Fundamental Science to Applications*; Bernier, P., Ed.; Elsevier: Amsterdam, 2000.

(4) Leclere, M. *Adv. Mater*. **1999**, *11*, 1491.

(5) McQuade, D. T.; Pullen, A. E.; Swager, T. M. *Chem. Rev*. **2000**, *100*, 2537.

(6) Zhou, Q.; Swager, T. M. *J. Am. Chem. Soc.* **1995**, *117*, 12593.

(7) Chen, L.; McBranch, D. W.; Wang, H. L.; Helgeson, R.; Wudl, F.; Whitten, D. G. *Proc. Natl. Acad. Sci. U.S.A.* **1999**, *96*, 12287.

(8) Gaylord, B. S.; Heeger, A. J.; Bazan, G. C. *Proc. Natl. Acad. Sci. U.S.A.* **2002**, *99*, 10954.

(9) Sato, T.; Jiag, D.-L. *J. Am. Chem. Soc.* **1999**, *121*, 10658.

(10) Wang, Y.; Erdogan, B.; Wilson, J. N.; Bunz, U. H. F. *Chem. Commun.* **2003**, 1624.

(11) Anzar, K.; Muller, S.; Hecht, S. *Chem. Commun.* **2005**, 584.

(12) Chen, L. H.; Xu, S.; McBranch, D.; Whitten, D. *J. Am. Chem. Soc.* **2000**, *122*, 9303.

(13) Lavigne, J. J.; Broughton, D. L.; Wilson, J. N.; Erdogan, B.; Bunz, U. H. F. *Macromolecules* **2003**, *36*, 7409.

(14) Burrows, H. D.; Lobo, V. M. M.; Pina, J.; Ramos, M. L.; Seixas de Melo, J.; Valente, A. J. M.; Tapia, M. J.; Pradhan, S.; Scherf, U. *Macromolecules* **2004**, *37*, 7425.

(15) Burrows, H. D.; Lobo, V. M. M.; Pina, J.; Ramos, M. L.; Seixas de Melo, J.; Valente, A. J. M.; Tapia, M. J.; Pradhan, S.; Scherf, U.; Hintschich, S. I.; Rothe, C.; Monkman, A. P. *Colloids Surf., A: Physicochem. Eng. Aspects* **2005**, *270*, 61.

(16) Yan, M.; Rothberg, L. J.; Kwock, E. W.; Miller, T. M. *Phys. Rev. Lett.* **1995**, *75*, 1992.

(17) Boissinot, Ho H. A. M.; Bergeron, M. G.; Corbell, G.; Dore, K.; Bondreau, D.; Leclere, M. *Angew. Chem., Int. Ed*. **2002**, *41*, 1548.

(18) Gaylord, B. S.; Heeger, A. J.; Bazan, G. C. *J. Am. Chem. Soc.* **2003**, *125*, 896.

(19) MacKnight, W. J.; Ponomarenko, E. A.; Tirrell, D. A. *Acc. Chem. Res.* **1998**, *31*, 781.

(20) Stork, M.; Gaylord, B. S.; Heeger, A. J.; Bazan, G. C. *Adv. Mater* **2002**, *14*, 361.

(21) Nilsson, P. G.; Wenuerstrom, H.; Lindman, B. *J. Phys. Chem.* **1983**, *87*, 1377.

(22) Menge, U.; Lang, P.; Findenegg, G. H.; Strunz, P. *J. Phys. Chem. B* **2003**, *107*, 1316.

(23) Wang, D. L.; Gong, X.; Heeger, P. S.; Rinins, F.; Bazan, G. C.; Heeger, A. J. *Proc. Natl. Acad. Sci. U.S.A.* **2002**, *99*, 49.

(24) Salager, J. L. *Surfactants, Types and uses*; FIRP Booklet no. 300A; University of Los Andes: Merido, Venezuela, 2002.

(25) . Shinzawa-ltoh, K.; Ueda, H.; Yoshikawa, S.; Aoyama, H.; Yamashita, E.; Tsukihara, T. *J. Mol. Biol.* **1995**, *246*, 572.

(26) Holmberg, K.; Jonsson, B.; Kronberg, B.; Lindman, B. *Surfactants and Polymers in Aqueous Solution*, 2nd ed.; Wiley: Chichester, U.K., 2003.

(27) Knaapila, M.; Almasy, L.; Garamus, V. M.; Pearson, C.; Pradhan, S.; Petty, C. M.; Scherf, U.; Burrows, H. D.; Monkman A. P. *J. Phys. Chem. B* **2006**, *110*, 10248.

(28) Knaapila, M.; Stepanyan, R.; Torkkeli, M.; Lyons, B. P.; Ikonen, T. P.; Almásy, L.; Foreman, J. P.; Serimaa, R.; Güntner, R.; Scherf, U.; Monkman A. P. *Phys. Rev. E* **2005**, *71*, 041802.

(29) Eastman, J. W.; Rehfeld, S. J. *J. Phys. Chem.* **1970**, *74*, 1438. (b) Schwarz, F. P.; Wasik, S. D. *Anal. Chem*. **1976**, *48*, 524.

(30) Bredas, J. L.; Cornil, J.; Heeger, A. *J. Adv. Mater*. **1996**, *8*, 447.

(31) Maroncelli, M.; Castner, E. W.; Bagchi, B.; Fleming, G. R. *Faraday Discuss. Chem. Soc.* **1988**, *85*, 199.

(32) Lakowicz, J. R. *Principles of Fluorescence Spectroscopy*, 2nd ed.; Kluwer Academic/Plenum Publishers: New York, 1999; Chapter 4, p 129.

(33) Liu, B.; Bazan, G. C. *J. Am. Chem. Soc.* **2004**, *126*, 1942.

(34) Zhou, W.; Wang, E. *J. Photochem. Photobiol. A: Chemistry* **1996**, *96*, 25.

(35) Achyuthan, K. E.; Bergstedt, T. S.; Chen, L.; Jones, R.; Kumaraswamy, M. S.; Kushon, S. A.; Ley, K. D.; Lu, L.; McBranch, D.; Mukundan, H.; Rininsland, F.; Shi, X.; Xia, W.; Whitten, D. G. *J. Mater. Chem.* **2005**, *15*, 2648.

(36) Conwell, E. M. *Phys. Rev. B* **1998**, *B57*, 14200.

(37) Wang, J.; Wang, D.; Miller, E. K.; Moses, D.; Bazan, G. C.; Heeger, A. J. *Macromolecules* **2000**, *33*, 5153.

(38) Torimura, M.; Kurata, S.; Yamada, K.; Yokomaku, T.; Kamagata, Y.; Kanagawa, T.; Kurane, R. *Anal. Sci.* **2001**, *17*, 155.

(39) Scherf, U.; List, E. J. W. *Adv. Mater*. **2002**, *14*, 477.

(40) Morris, J. V.; Mahaney, M. A.; Huber, J. R. *J. Phys. Chem.* **1976**, *80*, 969.

(41) Gratton, E.; Beechem, J. *Globals WE;* The Laboratory for Fluorescence Dynamics, University of Illinois at Urbana-Champaign: Urbana-Champaign, IL, 2005.